

Properties and Prospects of the Electron Doped Manganite $\text{La}_{1-x}\text{Ce}_x\text{MnO}_3$

Steffen Wirth, Chiranjib Mitra* and Pratap Raychaudhuri**

Mixed-valence manganese oxides $R_{1-x}A_x\text{MnO}_3$ (R = rare-earth cation, A = alkali or alkaline-earth cation) have been heavily investigated in recent years [1,2]. They show a variety of interesting crystallographic, electronic and magnetic properties one of which is the magnetoresistance. The latter effect may become extraordinary large (so-called colossal magnetoresistance, CMR) for temperatures around the ferromagnetic transition temperature T_C . Below T_C the mixed-valence manganites most commonly behave as ferromagnetic metals. This behavior becomes obvious, e.g., if trivalent La in the parent compound LaMnO_3 is substituted by divalent Ca: the missing electron produces a hole by driving the Mn^{3+} into the Mn^{4+} state. The crystal field interactions split the d -orbitals of Mn into t_{2g} and e_g orbitals. Hence, the e_g orbital is occupied by one electron in case of Mn^{3+} and is empty for Mn^{4+} which makes the former subject to Jahn-Teller distortion whereas the latter is not.

From this point of view, one may ask whether it is also possible to induce electron doping by substitution of R by a tetravalent element A . (e.g. Ce). A tetravalent element is expected to drive the compound into a mixture of Mn^{3+} and Mn^{2+} valencies induced by electron doping. There exists an inherent symmetry between Mn^{4+} and Mn^{2+} as both are non-Jahn-Teller ions. In addition, we found that $\text{La}_{0.7}\text{Ca}_{0.3}\text{MnO}_3$ and $\text{La}_{0.7}\text{Ce}_{0.3}\text{MnO}_3$ both have a Curie temperature of $T_C \approx 250$ K. Having both electron as well as hole-doped ferromagnetic manganites may open up very interesting applications in the emerging field of spintronics. Beyond the phenomenon of colossal MR, novel properties arising from the interplay of spin, charge and orbital coupling and the competition of closely related energy scales make these manganites fascinating materials.

The Ce-doped manganite $\text{La}_{1-x}\text{Ce}_x\text{MnO}_3$ has been reported to be a good candidate to induce electron doping on the manganese site [3,4]. As a prerequisite, single phase material is required which could only be prepared in thin film form so far [5]. The precursor material $\text{La}_{1-x}\text{Ce}_x\text{MnO}_3$ with $0 \leq x \leq 0.3$ was prepared by a solid state reaction

route and used as targets in the subsequent pulsed laser deposition (PLD). Thin epitaxial films were deposited on LaAlO_3 or SrTiO_3 substrates. A low oxygen pressure of 10 Pa was applied during film growth. This proved to be crucial to avoid over-oxygenation of the manganite films (it is well known that excess oxygen induces hole doping [2]). X-ray analysis was conducted to ensure the single phase nature of the films.

The sample magnetization was measured by using a Quantum Design superconducting quantum interference device (SQUID). Subsequently, the films were patterned into Hall bars for transport measurements by photolithography and wet chemical etching. This also enabled a film thickness determination, $d \approx 50$ nm, by Atomic Force Microscopy. The magnetization measurements for $\text{La}_{1-x}\text{Ce}_x\text{MnO}_3$ for $0 \leq x \leq 0.3$ are summarized in Fig. 1. The evolution of the magnetic moment M as well as of the Curie temperature T_C are evident. These data emphasize the high quality of the films.

It is well known that Ce can exist in two valence states, Ce^{3+} and Ce^{4+} , and therefore, we first need to establish that Ce-substitution indeed induces electron doping. We performed X-ray absorption spectroscopy (XAS) on thin films of $\text{La}_{0.7}\text{Ce}_{0.3}\text{MnO}_3$ [6]. XAS at the rare-earth $M_{4,5}$ and

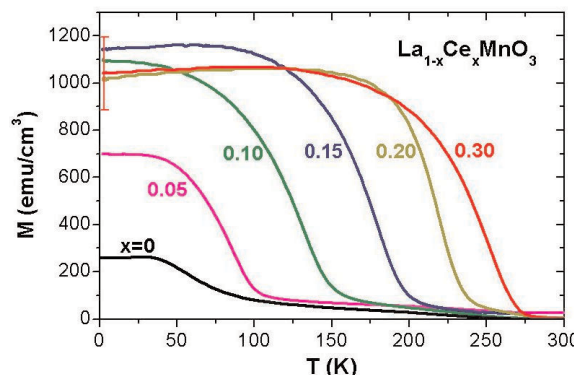


Fig. 1: Temperature dependence of the magnetization of thin film samples $\text{La}_{1-x}\text{Ce}_x\text{MnO}_3$ with $0 \leq x \leq 0.3$. The nominal Ce-doping x for the different samples is indicated. An error bar for the sample with $x = 0.3$ at low temperature is shown.

3d transition metal $L_{2,3}$ threshold is known to be highly sensitive to valence states. For the investigated samples $\text{La}_{0.7}\text{Ce}_{0.3}\text{MnO}_3$ a *pure* Ce(IV) valence state was evident. The existence of Ce(IV), however, still does not confirm that the sample is electron doped. In the past it has been shown that oxygen non-stoichiometries may be present in the manganites which may influence the doping level decisively [5]. Thus, to conclusively establish that it is indeed an electron-doped system one has to search for a corresponding replacement of Mn^{3+} by Mn^{2+} as well. We have measured the Mn- $L_{2,3}$ XAS spectra to investigate the valence state of Mn in the ground state. Fig. 2 shows the Mn- $L_{2,3}$ spectra of $\text{La}_{0.7}\text{Ce}_{0.3}\text{MnO}_3$ and – for comparison – of MnO_2 , LaMnO_3 and MnO for Mn^{4+} , Mn^{3+} and Mn^{2+} references, respectively. It is well known [7-9] that an increase of the metal ion valence by one results in

shift of the $L_{2,3}$ XAS spectra to higher energy by about 1 eV or more. In Fig. 2 we can see a shift towards higher energy from bottom to top in a sequence of increasing Mn valence from Mn^{2+} (MnO) to Mn^{3+} (LaMnO_3) and further to Mn^{4+} (MnO_2). In comparison to undoped LaMnO_3 , in $\text{La}_{0.7}\text{Ce}_{0.3}\text{MnO}_3$ we can see new and sharp low energy structures at nearly the same energy position as in the MnO spectrum. These sharp structures at around 642 eV are a reliable hallmark of the appearance of a divalent Mn state since they are hardly smeared by background or other structures. The observed spectral features indicate the existence of a Mn^{2+} component in addition to Mn^{3+} in the single phase $\text{La}_{0.7}\text{Ce}_{0.3}\text{MnO}_3$ compound. In order to estimate the Mn^{2+} content, the *normalized* spectrum of LaMnO_3 has been subtracted from that of $\text{La}_{0.7}\text{Ce}_{0.3}\text{MnO}_3$ (the resultant difference spectrum is labeled “difference” in Fig. 2). The main structures of the difference spectrum are found at the same energy position as the prominent features of the MnO spectrum (as indicated by the vertical line in Fig. 2 and the overall appearance of the difference and the MnO spectra is very similar. However, the difference spectrum in its details is not exactly the same as that of MnO . Subtle distinctions are to be expected because of the difference in the local symmetry of Mn in these two compounds. Moreover, minority spin carriers (see below) at the Fermi energy E_F may appear which may possibly lead to an intermediate spin state.

The content of Mn^{2+} was estimated to about 20%. The lower Mn^{2+} content compared to the nominal 30% Ce-doping could be caused by a slight over-oxygenation of the sample.

Magnetoresistivity and Hall measurements were conducted on the metallic-like samples $x = 0.15, 0.20$ and 0.30 for temperatures $5 \text{ K} - 300 \text{ K}$. As the most important result, all curves measured at $T < T_C$ show a negative high-field slope [10]. Hence, the main charge carriers are electrons, a finding in agreement with the XAS measurements. An analysis of the Hall resistivity, however, showed that it cannot be described by the simple assumption [11] of a spherical Fermi surface with only one type of charge carriers [10]. This situation is very similar to the Ca-doped manganites [12-14] where it is discussed in terms of charge carrier compensation due to a majority spin band consisting of hole and electron Fermi surfaces [15].

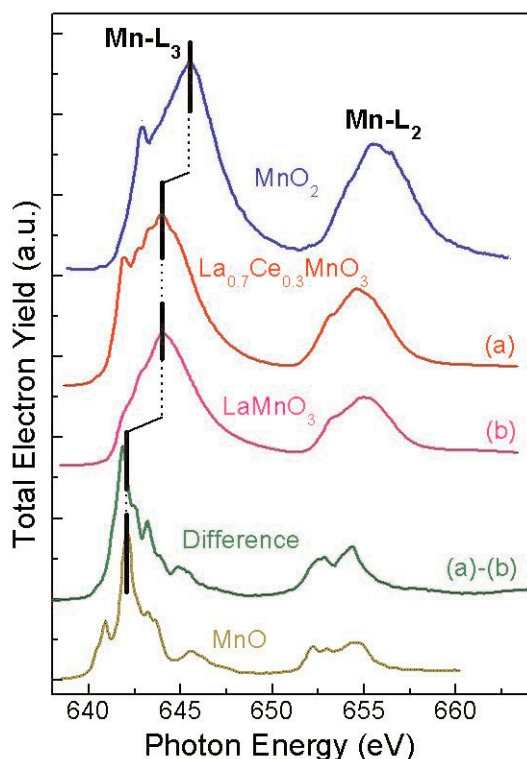


Fig. 2: Mn- $L_{2,3}$ XAS spectra of $\text{La}_{0.7}\text{Ce}_{0.3}\text{MnO}_3$. In addition, spectra of MnO_2 , LaMnO_3 (b) and MnO for Mn^{4+} , Mn^{3+} and Mn^{2+} references, respectively, are shown. The curve labeled “difference” (a)-(b) is the difference between the $\text{La}_{0.7}\text{Ce}_{0.3}\text{MnO}_3$ and the LaMnO_3 spectra. In comparison to the MnO spectrum, this difference curve clearly indicates the existence of Mn^{2+} in $\text{La}_{0.7}\text{Ce}_{0.3}\text{MnO}_3$ samples.

From the magnetization and resistance measurements the phase diagram of $\text{La}_{1-x}\text{Ce}_x\text{MnO}_3$ is constructed, see Fig. 3. The transition temperature between the ferromagnetic (FM) and the paramagnetic state is determined from T_C (marked by Δ) as well as from temperature T_P (\times in Fig. 3) at which the resistance assumes its maximum in case of the metallic samples. At low temperatures, i.e. in their ground state, samples with nominal doping $x \leq 0.10$ behave as ferromagnetic insulators whereas doping $x \geq 0.15$ results in FM metallic materials. This phase diagram is fascinatingly similar to the one reported [16] for the Ca-doped manganite; a similarity that could not be expected due to the different ionic radii of Ca and Ce.

Having both electron- and hole-doped manganites novel electronic devices can be realized. Trilayer tunnel junctions $\text{La}_{0.7}\text{Ce}_{0.3}\text{MnO}_3/\text{SrTiO}_3(50\text{\AA})/\text{La}_{0.7}\text{Ca}_{0.3}\text{MnO}_3$ were grown by PLD [4]. In the following the magnetotransport properties of such devices are discussed [17].

Fig. 4a shows the magnetic field dependence of the current versus voltage (I - V) curve across the tunnel junction measured in the CPP geometry at 300 K. We do not see a significant TMR, as expected, since at this temperature both $\text{La}_{0.7}\text{Ce}_{0.3}\text{MnO}_3$ and $\text{La}_{0.7}\text{Ca}_{0.3}\text{MnO}_3$ are paramagnetic semiconductors and the device behaves like a rectifying diode. However, in a field of 7.5 T the spin disorder scattering of a single layer is reduced and the in-plane MR is quite large [2].

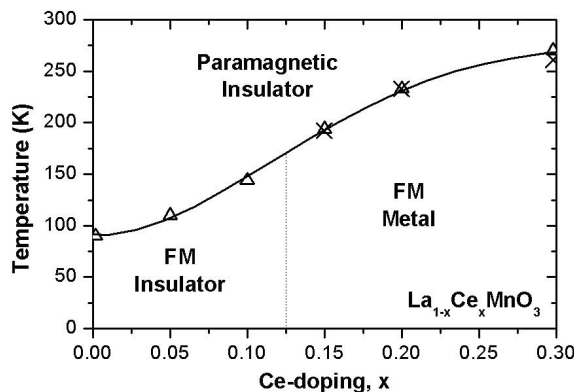


Fig. 3: Magnetic phase diagram of $\text{La}_{1-x}\text{Ce}_x\text{MnO}_3$ in the doping range $0 \leq x \leq 0.3$. The transition from ferromagnetic (FM) to para-magnetic behavior was determined from T_C (Δ) as well as from the temperature T_P (\times) at which the maximum resistivity of the metallic samples occurs. Note the striking similarity of the phase diagrams for Ce- and Ca-doped manganites

In Fig. 4b is presented the magnetic field dependence of the tunneling I - V curve taken at 100 K in zero field and in a field of 2 T. The field dependence (both positive and negative bias) clearly shows a bias dependent MR. A bias voltage V_b on a metallic tunnel junction shifts the Fermi levels of the two electrodes by eV_b . The tunneling of electrons across an insulating barrier, however, occurs at equal energy levels. Hence, the tunneling probabilities for the two different magnetization orientations of the electrodes (parallel or antiparallel) depends sensitively on the details of the spin-up and spin down DOS in the two electrodes. Moreover, small changes in the relative energies of the

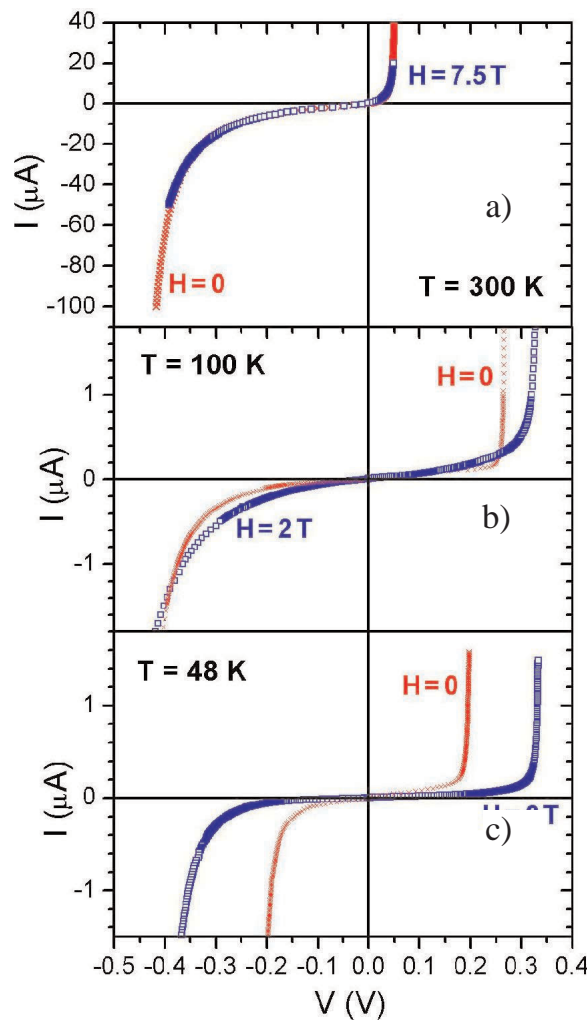


Fig. 4: a) The tunneling I - V characteristics of the trilayer junction, taken at 300 K, in zero field and in an in-plane field of 7.5 T. (b) The same as before, taken at 100 K, in zero field and in a field of 2 T. (c) The same as above, at 48 K.

$t_{2g}\downarrow$ and $e_g^2\uparrow$ bands due to V_b may change their occupancy which may also result in a bias dependent crossover. Here, a detailed understanding can emerge only when the DOS in $\text{La}_{0.7}\text{Ce}_{0.3}\text{MnO}_3$ is known in sufficient detail.

The field dependence of the I - V curves taken at 48 K (Fig. 4c) does not show any bias dependence. Here, the positive tunelling magnetoresistance (TMR) is intriguing. The conducting $e_g\uparrow$ band is energetically higher than the localized t_{2g} in a (nearly) cubic crystal field by about $\Delta_{cf} \sim 1.8$ eV [2]. The e_g band splits further due to Jahn-Teller distortion into two sub-bands which are separated by the Jahn-Teller splitting energy, $\delta_{JT} \sim 1.2$ eV. Jahn-Teller distortion also causes a splitting of the t_{2g} band by δ_{JT}^* . Moreover, Hund's rule coupling U_H removes the spin degeneracy in the ferromagnetic state ($U_H \sim 1.2$ eV [2]). The Mn-3d spin dependent density of states (DOS) of $\text{La}_{0.7}\text{Ca}_{0.3}\text{MnO}_3$ at low temperature is sketched in Fig. 5a. In hole doped manganites like $\text{La}_{0.7}\text{Ca}_{0.3}\text{MnO}_3$ (which have 0.7 electrons in the e_g band) the conduction electrons predominantly occupy the lowest sub-band $e_g^1\uparrow$. Consequently, the electrons at E_F are majority spin carriers in the hole doped manganites.

In $\text{La}_{0.7}\text{Ce}_{0.3}\text{MnO}_3$ there is clear evidence for electron doping on the Mn-site. Hence, the $e_g^1\uparrow$ sub-band is completely filled. For the remaining additional (doped) electrons two scenarios are possible: i) weak Hund's rule coupling $U_H < \Delta_{cf} + \delta_{JT}$ and ii) strong Hund's rule coupling $U_H > \Delta_{cf} + \delta_{JT}$. Only in the first case, $t_{2g}\downarrow$ is energetically lower than $e_g^2\uparrow$ and the former will get partially filled (Fig. 5b). The compound will be a minority spin carrier ferromagnet in an intermediate spin state. In the second case, the remaining electrons will occupy the $e_g^2\uparrow$ sub-band resulting in a majority spin carrier ferromagnet in high spin state. The observation of a positive TMR in the tunnel junctions at low temperature definitely favors the first scenario with antiparallel spins at E_F for fields high enough to align the magnetizations within the two ferromagnetic layers (cf. Fig. 5a and b). This result is supported by the known energy values given above. Band structure calculations [18] also predict the near-degeneracy of the energy positions of the $e_g^2\uparrow$ and the $t_{2g}\downarrow$ sub-bands. The minority spin character and the related intermediate spin state observed in

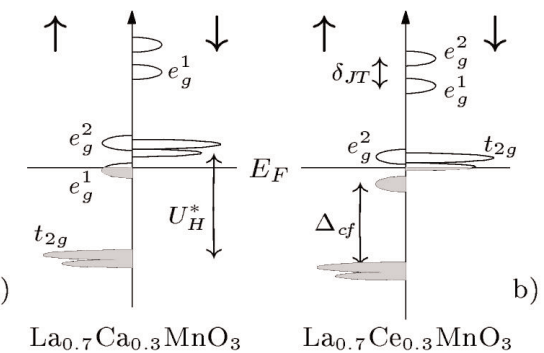


Fig. 5: Schematic diagram of spin dependent (large arrows) density of states of (a) the Ca and (b) the Ce-doped compounds at low temperature. For the Ce-doped compound, panel (b) depicts the case of the level $t_{2g}\downarrow$ being energetically lower than $e_g^2\uparrow$ resulting in a minority spin carrier state. For tunneling, the diagram correspond to the high field case, i.e., aligned magnetizations within the two ferromagnetic layers. This results in an increased resistance due to opposite spin states at E_F .

$\text{La}_{0.7}\text{Ce}_{0.3}\text{MnO}_3$ are intriguing. Due to the usually large on-site Hund's rule coupling this is rarely observed in manganese compounds where Mn is in the divalent state.

In conclusion, we reported on the magnetic and transport properties of $\text{La}_{1-x}\text{Ce}_x\text{MnO}_3$ with $0 \leq x \leq 0.30$. Conclusive evidence for electron doping in these materials (at least for $0.15 \leq x \leq 0.30$) from XAS and Hall measurements is presented. Having an electron-doped ferromagnetic counterpart to the well-known hole-doped manganites opens up a vast field of possibilities for applications and research alike. The magnetotransport properties of a tunnel junction made of electron and hole doped manganites led to the conclusion of minority spin carrier transport in $\text{La}_{0.7}\text{Ce}_{0.3}\text{MnO}_3$. This is of fundamental interest to understand the interplay of the Hund's rule coupling energy with other energy scales such as Jahn-Teller energy and crystal field energy in doped manganites. We believe that this result may open up an alternative approach towards *spintronics*.

This work was made possible only by strong collaborations: P.M. Oppeneer, K. Dörr, K.-H. Müller and L. Schultz at the IFW Dresden; Z. Hu, S.I. Csiszar and L.H. Tjeng at the University of Cologne and support by the Synchrotron Radiation Research Center in Taiwan.

References

- [1] S. Jin, T. H. Tiefel, M. McCormack, R. A. Fastnacht, R. Ramesh and L. H. Chen, *Science* **264**, 413 (1994).
- [2] J. M. D. Coey, M. Viret and S. von Molnár, *Adv. Phys.* **48**, 167 (1999).
- [3] P. Mandal and S. Das, *Phys. Rev. B* **56**, 15073 (1997).
- [4] C. Mitra *et al.*, *Appl. Phys. Lett.* **79**, 2408 (2001).
- [5] P. Raychaudhuri *et al.*, *J. Appl. Phys.* **86**, 5718 (1999).
- [6] C. Mitra, Z. Hu, P. Raychaudhuri, S. Wirth, S. I. Csiszar, H. H. Hsieh, H.-J. Lin, C. T. Chen and L. H. Tjeng, *Phys. Rev. B*, in print.
- [7] C. T. Chen and F. Sette, *Phys. Scripta T* **31**, 119 (1990).
- [8] Z. Hu *et al.*, *Chem. Phys.* **232**, 63 (1998).
- [9] Z. Hu *et al.*, *Phys. Rev. B* **61**, 3739 (2000).
- [10] P. Raychaudhuri, C. Mitra, P. Mann and S. Wirth, *J. Appl. Phys.*, in print.
- [11] C. M. Hurd, *The Hall Effect in Metals and Alloys* (Plenum, New York, 1972).
- [12] P. Matl, N. P. Ong, Y. F. Yan, Y. Q. Li, D. Studebaker, T. Baum and G. Doubinina, *Phys. Rev. B* **57**, 10248 (1998).
- [13] G. Jacob, F. Martin, W. Westerburg and H. Adrian, *Phys. Rev. B* **57**, 10252 (1998).
- [14] S. H. Chun, M. B. Salomon and P. D. Han, *J. Appl. Phys.* **85**, 5573 (1999).
- [15] W. E. Pickett and D. J. Singh, *Phys. Rev. B* **53**, 1146 (1996).
- [16] P. Schiffer, A. P. Ramirez, W. Bao and S.-W. Cheong, *Phys. Rev. Lett.* **75**, 3336 (1995).
- [17] C. Mitra, P. Raychaudhuri, K. Dörr, K.-H. Müller, L. Schultz, P. M. Oppeneer and S. Wirth, *Phys. Rev. Lett.* **90**, 017202 (2003).
- [18] S. Satpathy, Z. S. Popovic and F. R. Vukajlovic, *Phys. Rev. Lett.* **76**, 960 (1996).

* present address: Dept. of Materials Science, University of Cambridge, Pembroke St, Cambridge, CB2 3QZ, UK

** Tata Institute of Fundamental Research, Homi Bhabha Road, Bombay 400 005, India